



Improved fucoxanthin and docosahexaenoic acid productivities of a sorted self-settling *Tisochrysis lutea* phenotype at pilot scale

Fengzheng Gao^{a,*}, Marta Sá^a, Iago Teles Dominguez Cabanelas^a, René H. Wijffels^{a,b}, Maria J. Barbosa^a

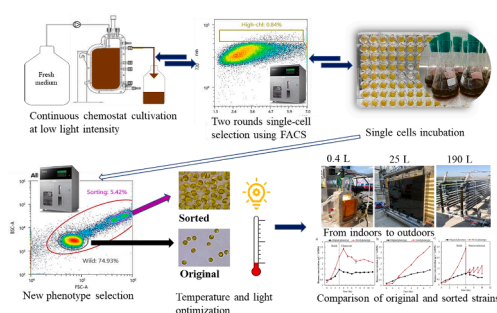
^a Wageningen University, Bioprocess Engineering, AlgaePARC, P.O. Box 16, 6700 AA Wageningen, Netherlands

^b Faculty Biosciences and Aquaculture, Nord University, N-8049 Bodo, Norway

HIGHLIGHTS

- Two rounds of directed evolution resulted in a novel *Tisochrysis lutea* phenotype.
- Stable phenotype after 15 months and contamination resistance in outdoor production.
- Fucoxanthin outdoor productivity was 3.1× higher than the original strain.
- Docosahexaenoic acid (DHA) outdoor productivity was 1.6× higher than original strain.
- Highest ever reported outdoor biomass, fucoxanthin and DHA productivities.

GRAPHICAL ABSTRACT



ARTICLE INFO

Keywords:

Fluorescence-activated cell sorting (FACS)
Fucoxanthin
High productivity
Robust new phenotype
Tisochrysis lutea

ABSTRACT

This work aimed to select a *Tisochrysis lutea* phenotype with higher biomass and fucoxanthin productivities using fluorescence-activated cell sorting (FACS). A novel phenotype was obtained after 2 rounds of selection, based on high-fucoxanthin fluorescence. The resulting phenotype forms cell aggregates, has no flagella, and was stable after 15 months. Optimal temperature (30 °C) and light (300 $\mu\text{mol m}^{-2} \text{s}^{-1}$) were obtained at laboratory scale, identical to the original strain. The biomass productivity was higher than the original strain: 1.9× at laboratory scale (0.4 L), and 4.5× under outdoor conditions (190 L). Moreover, compared to the original strain, the productivity of fucoxanthin increased 1.6–3.1× and docosahexaenoic acid 1.5–1.9×. These are the highest ever reported outdoor productivities, obtained with a robust new phenotype from a *T. lutea* monoculture isolated with FACS without genetic manipulation. The resulting phenotype shows high potential for industrial production.

1. Introduction

In recent years, *Tisochrysis lutea* has obtained high attention due to its wide applications in aquaculture and high content of valuable compounds, such as fucoxanthin (Fx) and docosahexaenoic acid (DHA). Fx is

a high-value compound with several biological properties, such as antioxidant, anti-obesity, and antidiabetic, which can be used as ingredient in cosmetics, pharmaceuticals, and nutraceuticals (Fung et al., 2013; Guedes et al., 2011; Maeda et al., 2018). The selling price of purified Fx varies considerably from 40 000 to 80 000 USD kg^{-1} ,

* Corresponding author.

E-mail address: fengzheng.gao@wur.nl (F. Gao).

<https://doi.org/10.1016/j.biortech.2021.124725>

Received 7 December 2020; Received in revised form 11 January 2021; Accepted 12 January 2021

Available online 18 January 2021

0960-8524/© 2021 The Author(s). Published by Elsevier Ltd. This is an open access article under the CC BY license (<http://creativecommons.org/licenses/by/4.0/>).

depending on the degree of purity and concentration in the final extract (Joel, 2016). The current Fx production uses edible brown seaweed as feedstock, despite their low Fx concentration (0.01 to 3.7 mg g⁻¹ dry weight (DW)) (Terasaki et al., 2012; Verma et al., 2017; Zailanie and Sukoso, 2014). Microalgae have up to 100 times more Fx than seaweeds (Lu et al., 2018). For example, Fx content in *T. lutea* was reported up to 20.3 mg g⁻¹ DW (Gao et al., 2020a).

DHA is a long-chain omega-3 fatty acid associated with numerous health benefits, such as promoting fetal development and improving the cardiovascular condition (Swanson et al., 2012). Currently, DHA is mainly extracted from cold-water oceanic fish, which is facing losses due to overfishing and global warming (Colombo et al., 2020). Besides Fx and DHA, *T. lutea* has also high contents of proteins and carbohydrates, which can also be developed as high-value products (da Costa et al., 2017; Ippoliti et al., 2016b).

Although the contents of these compounds in *T. lutea* are high, the productivity is still relatively low. For example, Fx and DHA productivities at laboratory scale were reported from 0.055 to 7.96 mg L⁻¹ d⁻¹ and 0.3 to 13.6 mg L⁻¹ d⁻¹, respectively (da Costa et al., 2017; Ishika et al., 2017; Liu et al., 2013; Sun et al., 2019). The productivity decreases from laboratory to industrial scale, and from indoors to outdoors, due to daily environmental fluctuations. Biomass productivity reached 1 g L⁻¹ d⁻¹ at laboratory scale under indoor conditions (Gao et al., 2020c) but was only 0.2–0.3 g L⁻¹ d⁻¹ in tubular photobioreactors (PBRs) operated inside a greenhouse in Almería, Spain (Ippoliti et al., 2016b, 2016a). It was even lower (40 mg L⁻¹ d⁻¹) in floating PBRs operated outdoors in Lingshui Bay, in Dalian, China (38°87'N, 121°55'E) (Zhu et al., 2019). Developing a robust *T. lutea* strain with high biomass, Fx, and DHA productivities under outdoor conditions is critical for commercial applications.

Efficient selection tools are necessary to obtain robust industrial strains. It has been shown that robust strains can be selected from microalgae monocultures (Picardo et al., 2013). Fluorescence-activated cell sorting (FACS) is a powerful tool that has been used widely in living microalgal cell monitoring and selection (Cabanelas et al., 2015, 2016; Gao et al., 2021; Pereira et al., 2011). Previous research studied the possibilities of using FACS for selection of different microalgal phenotypes, resulting in improved performances such as doubled triacylglycerol productivity, doubled lipid content, and increased β -carotene content (Cabanelas et al., 2016; Mendoza et al., 2008; Yen Doan and Obbard, 2011). A high throughput method for Fx and lipids quantification using FACS has been developed for *T. lutea* by Gao et al. (2020b), and is used in this work to select cells with high Fx and/or lipids.

In the present study, continuous chemostat experiments were operated under low light intensity (50 $\mu\text{mol m}^{-2} \text{s}^{-1}$) to induce Fx accumulation. Following, single cells with high Fx content were sorted using FACS and used to inoculate a new chemostat. The chemostat cultivation and FACS selection were repeated until a new phenotype was obtained. In total, 2 rounds of FACS selection were performed to obtain an improved phenotype. Temperature and light intensity for the cultivation of the selected *T. lutea* were optimized using continuous experiments. Finally, the performance (growth, fucoxanthin and DHA production) of the culture with improved phenotype was compared with the original culture using different systems (0.4, 25, and 190 L), indoors and outdoors.

2. Materials & methods

2.1. Strain and maintenance conditions

Tisochrysis lutea strain (previously identified as *Isochrysis galbana* T-Iso or *Isochrysis* sp.) (Bendif et al., 2013), and the commercial culture medium stock NutriBloom Plus were kindly provided by NECTON, S.A. (Olhão, Portugal). The culture medium was prepared with natural seawater (salinity \approx 33 ppt) from the North Sea (the Netherlands),

enriched with 2 mL L⁻¹ of the NutriBloom Plus stock and 40 mM NaNO₃, with a final pH of 8.0 (containing 20 mM HEPES). For maintenance of the original and sorted *T. lutea*, cultures were inoculated in 250 mL Erlenmeyer flasks with 100 mL medium. The flasks were placed in incubators (Infors, Switzerland) at 25 °C, a light intensity of approximately 140 $\mu\text{mol m}^{-2} \text{s}^{-1}$, 18/6h day/night cycle, with 2.0% CO₂, and under constant agitation of 125 rpm.

2.2. Reactor setup and cell sorting

2.2.1. Continuous cultivation for fucoxanthin accumulation

The original strain was cultivated using flat-panel photobioreactors (PBRs; Algaemist, light path 14 mm, cultivation volume 0.4 L) (Hulatt et al., 2017), at 50 $\mu\text{mol m}^{-2} \text{s}^{-1}$ and under continuous chemostat mode with a fixed dilution rate (0.5 d⁻¹). These cultivation conditions were previously shown to result in the highest Fx content (16.8 mg g⁻¹ DW) (Gao et al., 2020a). The temperature was controlled using a water-jacket connected to the heating/cooling system, and the pH was kept constant at 8.0 by CO₂ injection. The culture was continuously aerated by filtered air at a rate of 0.4 L min⁻¹.

2.2.2. Cell sorting

Cell sorting was performed after at least 3 replacements of the cultivation volume (1200 mL in total) by fresh medium. A Sony Cell Sorter SH800S with a 100 μm microfluidics sorting chip (LE-C3210, Sony, Japan) was used for single-cell fluorescence measurement and cell sorting. A 1.5 mL Eppendorf tube containing the culture with an optical density at 750 nm (OD₇₅₀) of 0.2 was placed in the sample chamber. Cells were selected from three different density plots (Fig. 1). A 488 nm laser was used to excite chlorophyll *a* and Fx (Gao et al., 2020b). Firstly, the backward scatter area (BSC-A) was plotted against the forward scatter area (FSC-A) to distinguish bacteria and other impurities from the microalgae. A gate was created to select only the microalgal cells (Fig. 1a). Next, the signals for FSC and BSC were plotted to select single cells. Finally, a gate was created in a BSC height versus area plot to include all cells. The single-cell fluorescence was collected from 100 000 events. A selection gate was created to select cells with high emission signals (top 0.8%) at 720 nm (Fig. 1b). From the selection gate, single cells were selected into a sterile 96-well plate, containing 100 μL sterile NutriBloom medium (4 mM nitrogen, pH 8.0). Each well contained 1 single cell. The 96-well plate was placed in a climate room at 25 °C, with a light intensity of approximately 40 $\mu\text{mol m}^{-2} \text{s}^{-1}$ and an 18/6h day/night cycle.

2.2.3. Incubation and re-sorting of the selected cells

A plate reader (Infinite M200, TECAN) was used to measure the OD₄₅₀ (for carotenoid content) (Mishra et al., 2012) and OD₇₅₀ of the 96-well plate after 10 days. More than 80% of the single cells can survive after sorting (Gao et al., 2020b). The surviving cells (Top 8 with high ratio of OD₄₅₀/OD₇₅₀) were transferred into 250 mL Erlenmeyer flasks with 100 mL medium and cultivated under the same conditions as described before. FACS was used to monitor the fluorescence emission at 720 nm of each selected strain during exponential growth. The selected strain was regrown in an Algaemist under chemostat mode. The steps of Sections 2.2.1 and 2.2.2 were repeated. After 2 rounds of FACS selection, a new population was found (Fig. 1c). FACS was used to select single cells from the gate with high fluorescence (sorting gate in Fig. 1c) to a 96-well plate. The selected cells were incubated and cultivated as described above. The DNA of the original and novel *T. lutea* was extracted using the dilution buffer in PhireTM Plant Direct PCR Master Mix kit. The polymerase chain reaction was performed using 18 s universal primers (R: GCTTTCGCAGTAGTTCGTCCT; F: CAAGTTTCTGCCCTATCAGCT); and the products were sent to Macrogen Europe B.V. for 18 s sequencing. The sequencing results were analysed by BLAST (basic local alignment search tool) in the NCBI database.

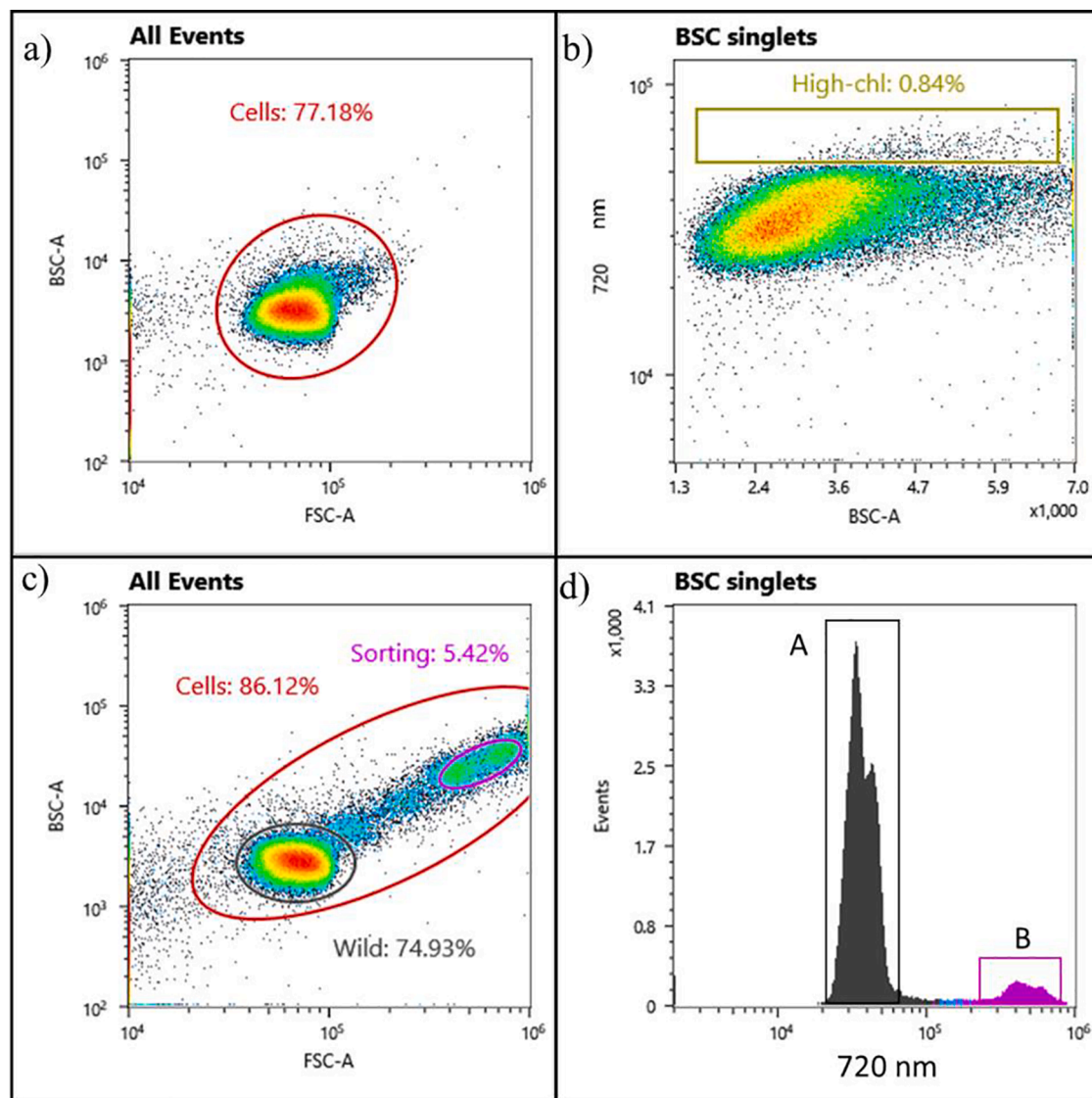


Fig. 1. Density and histogram plots in FACS selection. a: Granularity (BSC-A) versus cell size (FSC-A) of the original *Tisochrysis lutea* population; b: Single-cell fluorescence of original *Tisochrysis lutea* at 720 nm. A gate was created for cell selection with high fluorescence (top 0.8% cells); c: Populations of original and novel *Tisochrysis lutea* phenotypes; d: Single-cell fluorescence of original and novel phenotypes at 720 nm. A: original *Tisochrysis lutea*; B: novel phenotype.

2.3. Process optimization

2.3.1. Temperature optimization

The novel *T. lutea* was inoculated in four Algaemists with an initial $OD_{750} \approx 0.25$. Algaemists were firstly operated in batch mode for 5 days, at 30 °C, with a light intensity of $300 \mu\text{mol m}^{-2} \text{s}^{-1}$, 18/6h day/night cycle, and a constant pH of 8.0. Then, the temperature was switched to 15.8, 20, 25, and maintained at 30 °C in one of the reactors. At the same time, the continuous turbidostat mode started with an $OD_{750} \approx 3.5$. The backlight intensity was kept constant ($\approx 15 \mu\text{mol m}^{-2} \text{s}^{-1}$) with the help of a black-sheet cover to avoid interference from the surrounding light. When the backlight intensity decreased below the set-point, due to the increase of biomass concentration, the dilution pump ran automatically to dilute the culture back to the initial biomass concentration. After 10 days of cultivation at steady state, the temperature of the Algaemist running at 30 °C was increased to 35 °C for 5 days.

The overflow culture was collected in a harvest vessel for all reactors at the same time every day for Fx and fatty acids measurement. The continuous turbidostat experiment lasted for 10 to 16 days to replace the culture by at least 3 cultivation volumes, except at 15.8 and 35 °C due to low growth rate or decreased biomass concentration.

2.3.2. Light intensity optimization

The novel *T. lutea* was inoculated as described in the previous section. For the first four days, the microalgae were cultivated in batch mode with an incident light intensity of $300 \mu\text{mol m}^{-2} \text{s}^{-1}$ under 18/6 day/night cycle. When biomass concentrations reached an $OD_{750} > 3$, the light intensities were changed to 50, 150, 300, and $500 \mu\text{mol m}^{-2} \text{s}^{-1}$. The chemostat experiments were started with a dilution rate of 0.40 d^{-1} at the time that light changed. The biomass was harvested for Fx measurement at the same time every day.

2.4. Comparison of original and novel phenotype in different cultivation systems

2.4.1. Comparison of original and novel phenotypes in Algaemist

The original and novel *T. lutea* were inoculated in Algaemists at 30 °C, with the light intensity of $300 \mu\text{mol m}^{-2} \text{s}^{-1}$, 18/6h day/night cycle, and a constant pH of 8.0. The Algaemists were firstly run at batch mode for 3 days, and then switched to continuous chemostat mode with a fixed dilution rate of 0.5 d^{-1} . Samples were harvested as described before.

2.4.2. Comparison of original and novel phenotypes in flat-panel photobioreactors

Original and novel *T. lutea* were inoculated in 25 L flat-panel PBRs (Algae-Germ), with an initial $OD_{750} \approx 0.25$, and operated at batch mode at 30 °C, with a continuous light intensity of $\approx 250 \mu\text{mol m}^{-2} \text{s}^{-1}$. The PBRs were operated in the greenhouse of AlgaePARC (51° 59' N, 5° 39' E, the Netherlands), with varying sunlight and constant artificial light supply with maximum of $\approx 800 \mu\text{mol m}^{-2} \text{s}^{-1}$. The PBRs with original and novel phenotypes were placed at similar positions to receive identical light supply. Samples (≈ 500 mL) were collected daily for Fx and fatty acids analysis.

2.4.3. Comparison of original and novel phenotype in tubular photobioreactors

The cultures of original and novel *T. lutea* in Algae-Germ PBRs were used as inoculation for pilot tubular PBRs (190 L). The tubular PBRs were operated outdoors in AlgaePARC, at a temperature of 27–30 °C controlled by a cooling-heating system. The medium was the same as described in 2.1; and the pH was kept constant at 8.0 by automatic CO_2 injection. The tubular PBRs were operated in batch mode for 6 days, and then switched to semi-continuous mode. The outdoor light intensity (from 5:30 am to 9:00 pm), reached a maximum of $\approx 1500 \mu\text{mol m}^{-2} \text{s}^{-1}$ at noon. The average daily light intensities were similar ($35\text{--}40 \text{ mol m}^{-2} \text{d}^{-1}$) during the semi-continuous cultivation period. Samples (≈ 500 mL) were collected daily at 10:00 am for Fx and fatty acids analysis. After sampling, dilution was performed to maintain a certain biomass concentration (1 g L^{-1} ash free dry weight, AFDW).

2.5. Daily measurement

The OD_{750} and quantum yield (QY) were measured according to the previous methods (Gao et al., 2020a). The novel *T. lutea* cells showed to be sensitive to the washing solution (0.5 M ammonium formate) and were disrupted after washing; therefore, both original and novel *T. lutea* cells were centrifuged (5 min, 15 °C, $4255 \times g$) without a washing step. The cell pellet was flushed with N_2 and stored at -20 °C. The stored samples were freeze-dried (Sublimator $2 \times 3 \times 3.5$, Zirbus Technology, the Netherlands) for 41 h. A small amount of each sample (5–10 mg) was weighted in a pre-weighted glass tube for later AFDW measurements. The weight of the glass tube with sample was also measured, and then placed in the oven under the following protocol: 105 °C for 1.5 h; 575 °C for 4 h; cooling down to 105 °C (≈ 4 h). Afterwards, the glass tube was removed from the oven and cooled down to room temperature in a desiccator for 2 h. Afterwards the glass tube weight was measured again (tube with ash). The AFDW is the difference between the weight of the tube with algae and the weight of the tube with ash.

2.6. Cell composition analysis

2.6.1. Fucoxanthin and fatty acids measurement

Fx and fatty acids were extracted and measured according to previously reported methods (Gao et al., 2020b, 2020a). The biomass used was ≈ 5 and ≈ 15 mg, higher than what was reported in previous methods, due to the presence of salt in the samples.

2.6.2. Carbohydrate analysis

The total carbohydrate content was analysed according to Dubois et al. (1956). Approximately 1 mg of freeze-dried biomass was weighted in an Eppendorf tube using an analytical balance. In addition, 1 mg of glucose was weighted as a positive control. Following, 0.5 mL of 2.5 M HCl was added and incubated in a boiling water bath for 3 h. During incubation, samples were vortexed every hour. Samples were cooled down to room temperature after incubation and centrifuged for 10 min at $1200 \times g$. The supernatant (50 μL) was transferred to a fresh glass tube. Afterwards, 450 μL of Mili-Q water and 500 μL 5% phenol solution was added to the glass tube. Furthermore, 2.5 mL of concentrated sulphuric

acid was added to the liquid surface and incubated for 10 min at room temperature. The samples were incubated in a 35 °C water bath for 30 min and vortexed every 5 min. Absorbance at 483 nm was measured in a TECAN M200 Plate Reader. A sample without glucose was prepared as blank. All measurements were performed in duplicate.

2.6.3. Protein analysis

Protein analysis was performed according to the Lowry method (LOWRY et al., 1951). A small amount of freeze-dried biomass (1–3 mg) was treated with 1 mL 0.4 M NaOH in an Eppendorf tube and incubated for 30 min at 100 °C in a heating block. The Eppendorf tube was centrifuged for 10 min at $1150 \times g$. The supernatant was diluted if needed. Standards were prepared using 0.4 M NaOH with concentrations of 0, 0.05, 0.1, 0.2, 0.4, 0.6, 0.8, 1.0, 1.2, 1.4 mg mL^{-1} . Standards and samples were pipetted (10 μL) into a 96-wells flat bottom transparent Greiner Bio-one microplate (#650201). Protein assay Reagent A (25 μL) and B (200 μL) (Bio-Rad Dc protein assay kit) were added to each well. The plate was covered with aluminum foil and incubated for 30 min at room temperature. The absorbance at 750 nm was measured in a TECAN M200 Plate Reader. Each measurement was repeated in triplicate. The protein content was calculated based on the standard curve.

2.7. Data calculation and analysis

2.7.1. Calculations

The growth rate (μ ; d^{-1}) in continuous chemostat or turbidostat experiments during steady-state was equal to the dilution rate D (d^{-1}); and was calculated according to Eq. (1);

$$\mu = D = V_h/V_R \quad (1)$$

where V_h (mL) was the volume of the daily harvest culture, and V_R (0.4 L) was the cultivation volume of the Algaemist.

The volumetric biomass productivity (P_X ; $\text{g L}^{-1} \text{d}^{-1}$ AFDW) in continuous chemostat or turbidostat experiments was calculated using Eq. (2);

$$P_X = C_x \times D \quad (2)$$

where C_x was the biomass concentration (g L^{-1} AFDW) at steady state, and D was the dilution rate (d^{-1}); and was given as an average productivity.

The growth rate (μ ; d^{-1}) in batch experiments was calculated according to Eq. (3);

$$\mu(\text{d}^{-1}) = \ln(\text{AFDW}_2/\text{AFDW}_1)/(t_2 - t_1) \quad (3)$$

where AFDW_2 and AFDW_1 were the AFDW at the end and start of the exponential growth phase. The time of exponential growth is represented by t_2 and t_1 .

The volumetric biomass productivity (P_X ; $\text{g L}^{-1} \text{d}^{-1}$ AFDW) in batch experiments was calculated using Eq. (4);

$$P_X = (\text{AFDW}_2 - \text{AFDW}_1)/(t_2 - t_1) \quad (4)$$

where AFDW_2 and AFDW_1 were the AFDW at the end and start of the exponential growth phase. The time of exponential growth is represented by t_2 and t_1 .

The growth rate (μ ; d^{-1}) in semi-continuous experiments was calculated according to Eq. (5);

$$\mu = (\text{AFDW}_1 - \text{AFDW}_0)/\text{AFDW}_0 \quad (5)$$

where AFDW_1 and AFDW_0 were the AFDW at the current and previous day.

The volumetric biomass productivity (P_X ; $\text{g L}^{-1} \text{d}^{-1}$ AFDW) in semi-continuous experiments was calculated using Eq. (6);

$$P_X = (\text{AFDW}_1 - \text{AFDW}_0)/(t_1 - t_0) \quad (6)$$

where AFDW_1 and AFDW_0 were the AFDW at the current and

previous day; $t_1 - t_0 = 1$.

The volumetric valuable compounds (Fx, lipids, DHA, carbohydrates, and proteins) productivity (P_C ; $\text{mg L}^{-1} \text{d}^{-1}$) was calculated using Eq. (7);

$$P_c = C_c \times P_X \quad (7)$$

where C_c was the compound concentration (mg g^{-1} AFDW) at steady state and P_X was the biomass productivity ($\text{g L}^{-1} \text{d}^{-1}$ AFDW); and was given as an average productivity.

2.7.2. Statistical analyses

The results were analysed based on the data from at least three different cultivation points. Experimental results were expressed as mean value \pm standard deviation (SD). Differences between groups were tested using the IBM® SPSS® Statistics software program (version 25). The relationship between variables was determined by one-way ANOVA at a significance level of 0.05 using a Duncan Post-Hoc test.

3. Results and discussion

3.1. Selecting novel *Tisochrysis lutea* phenotype

Strain selection is critical in improving growth and productivity. In this section, continuous chemostat experiments were conducted with low light intensity ($50 \mu\text{mol m}^{-2} \text{s}^{-1}$), which is known to induce Fx production in *T. lutea* (Gao et al., 2020b). After at least 3 rounds of culture replacement in the photobioreactor, an increasing number of cells with high-Fx content is expected inside the photobioreactor. These cells have an advantage under low light conditions, while the cells (with low Fx), which do not grow that fast under these conditions, will be washed out of the reactor due to continuous operation (chemostat). Following, FACS was used to select single *T. lutea* cells with high Fx fluorescence (top 0.8%, Fig. 1b). To increase the chance of obtaining an improved strain, one selected single cell was regrown for another round of continuous cultivation, followed by FACS selection, until a new phenotype was obtained.

The performance of single cells ($n = 96$) selected from the first round of continuous chemostat cultivation was similar to the original cells based on growth and FACS analysis. One selected cell (among 96) obtained from the second selection round led to a different population (Fig. 1c) with a significantly higher fluorescence (Fig. 1d; gate B) at 720 nm than the original population (Fig. 1d; gate A). In total, the time required to develop this new population was approximately 6 months, including 2 rounds of continuous cultivation and 2 rounds of FACS selection. In general, several rounds of sorting are needed to obtain an improved phenotype (Pereira et al., 2018). For instance, an improved *Chlorococcum littorale* strain with doubled triacylglycerol productivity was obtained after 5 rounds of sorting for lipid-rich cells (Cabanelas et al., 2016). An *Euglena gracilis* mutant with 40% more lipid content was obtained after 4 rounds of sorting for top 0.5% lipid-rich cells (Yamada et al., 2016). Two *Tetraselmis suecica* strains that produced more neutral lipids (increases of 114 and 123%) were isolated after 5 rounds of selection for cells presenting increased lipid fluorescence using FACS combined with mutagenesis (Lim et al., 2015).

To obtain a single clone from the new population, FACS was also used as a tool to isolate pure cells from the new population by sorting one single cell to each well of the 96-well plate. The same procedure was done for the original strain for comparison. After 10 days of incubation, the original *T. lutea* cells were homogeneously distributed in the whole well, whereas single cells selected from the new population aggregated at the bottom of the well. The aggregated cells were considered as a novel phenotype. The colour of the novel phenotype culture incubated in the 96-well plate and grown in Algaemist was the same as the original phenotype. Microscopic observation showed that the original cells swam individually by means of two flagella while the novel phenotype cells were motionless and had no flagella. Due to the aggregated population,

more than one cell passed through the FACS detector, which resulted in the higher FSC/BSC signal and fluorescence (Fig. 1c, d). The obtained novel *T. lutea* has a strong self-settling ability. A 90% concentration was observed by settlement within 60 min in a 50 mL Greiner falcon tubes with 50 mL culture without mixing, indicating a potentially lower harvesting cost.

The 18 s sequence of the novel phenotype showed a 100% overlap with the original phenotype, and BLAST with NCBI database as *T. lutea*. The novel strain has been cultivated for 15 months in different cultivation systems, always showing a stable phenotype.

3.2. Cultivation parameters optimization

The optimal growth parameters of the novel *T. lutea* may differ from the original strain. Since temperature and light are two of the most important parameters affecting microalgal growth, these two parameters were optimized in Algaemists using continuous turbidostat or chemostat mode.

3.2.1. Effect of temperature on growth, fucoxanthin and fatty acids production

The biomass concentration was constant during continuous turbidostat cultivation for all temperatures except at 35 °C, which showed a sharp decrease (Fig. 2a). The growth rate increased from 0.05 to 0.41 d^{-1} with increasing temperature from 15.8 to 30 °C ($p < 0.05$). The optimal temperature was 30 °C, which was the same as reported for the original strain (Gao et al., 2020b). The biomass productivity followed the same trend as the growth rate, highest at 30 °C and lowest at 15.8 °C. Although the mean growth rate (first 3 days after temperature switch) and biomass productivities at 35 °C were higher than at 15.8 °C, they decreased to 0 after 3 days of cultivation. The QY (Fig. 2b; Table 1) at 25 and 30 °C (0.71) was significantly higher than at 15.8, 20 and 35 °C (0.53–0.68; $p < 0.05$), also in line with the growth rate and biomass productivity.

The Fx content showed no obvious trends from 15.8 to 30 °C, ranging from 3.69 to 4.68 mg g^{-1} (Table 1), in line with reported findings at different temperatures from 16.5 to 30 °C (Gao et al., 2020a). The Fx content at 35 °C was significantly lower than at other temperatures due to relatively high light per cell resulting from the low biomass concentration ($p < 0.05$). The trends of the total fatty acids (TFA) and DHA contents were similar to Fx. The TFA and DHA content ranged from 73.92 to 110.37 mg g^{-1} AFDW and 8.67 to 14.33 mg g^{-1} AFDW (Table 1). The Fx productivity was the highest at 30 °C, similar to that at 25 °C, and 7.9-, 1.6-, and 3.6-fold higher than the ones measured at 15.8, 20, 35 °C, respectively. The DHA and TFA productivities showed similar trends as Fx. All these showed that 30 °C was the optimal temperature for growth and valuable compounds production of the novel *Tisochrysis lutea*.

3.2.2. Effect of light on growth, fucoxanthin and fatty acids production

T. lutea is a brown microalga that can change pigmentation in a short time as a response to changes in light intensity. The changes in pigmentation will affect the backlight intensity, therewith affecting continuous turbidostat operation. Therefore, continuous chemostat experiments (Fig. 2c) were performed for optimizing light intensity with a fixed dilution rate.

The growth rates were therefore similar, from 0.39 to 0.42 d^{-1} , for all chemostat experiments (Table 2). The biomass concentration during steady state increased from 0.67 to 2.75 g L^{-1} AFDW with increasing light from 50 to 500 $\mu\text{mol m}^{-2} \text{s}^{-1}$ (Table 2). At 500 $\mu\text{mol m}^{-2} \text{s}^{-1}$ the biomass concentration decreased gradually, not reaching a steady state, due to photoinhibition (Suknik et al., 1993). This was also indicated by the lower QY (0.69) compared to other light intensities (Fig. 2d; Table 2). The biomass productivity increased from 0.28 to 1.12 $\text{g L}^{-1} \text{d}^{-1}$ AFDW as increasing light from 50 to 500 $\mu\text{mol m}^{-2} \text{s}^{-1}$.

The Fx content increased from 2.25 to 6.66 mg g^{-1} AFDW with

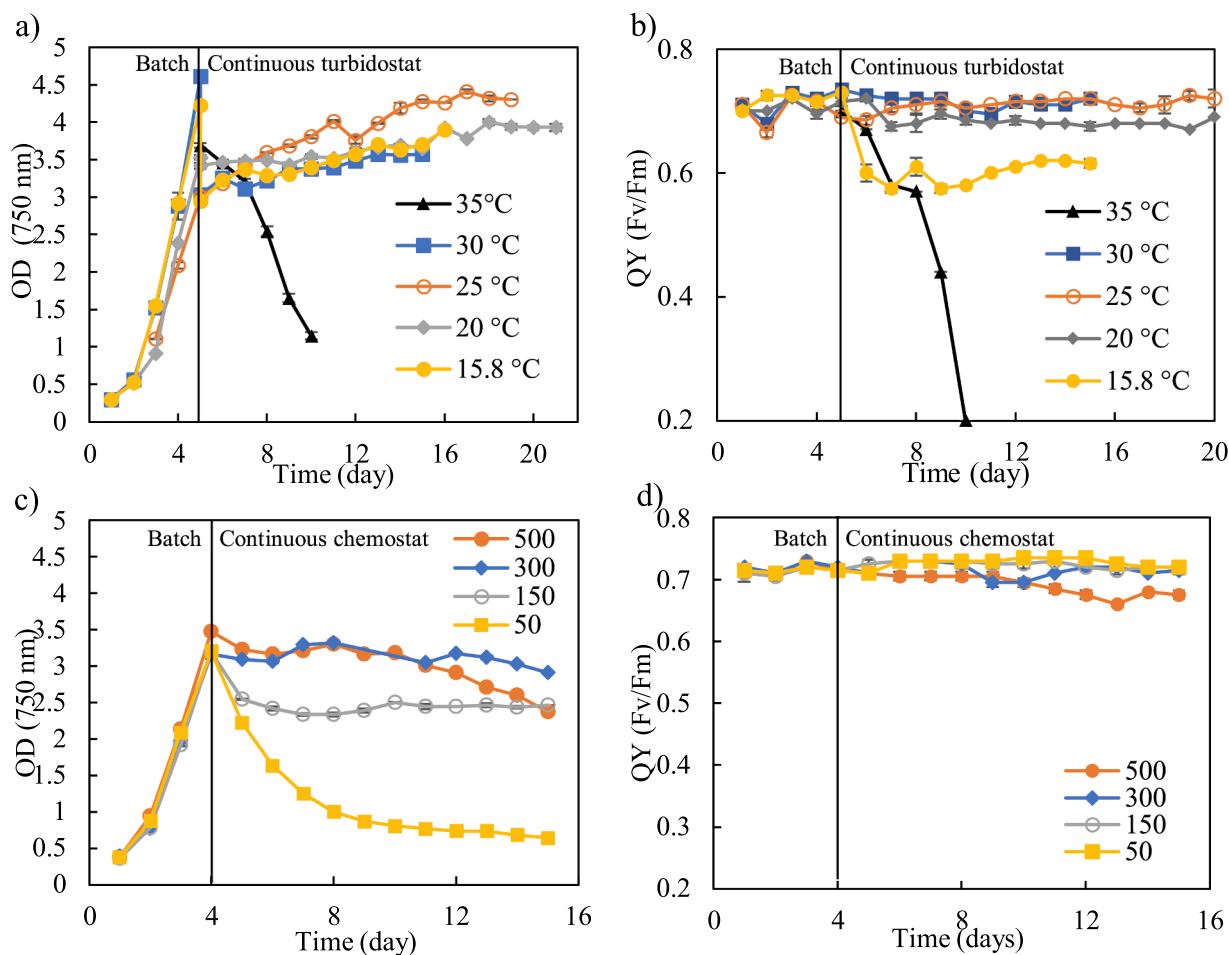


Fig. 2. Growth curves and quantum yield dynamics of the novel *Tisochrysis lutea*. a: Growth curves at different temperatures; b: Quantum yield dynamics at different temperatures; c: Growth curves at different light intensities; d: Quantum yield dynamics at different light intensities. Note: Growth and biomass composition analysis time points: day 7–21 for 15.8–30 °C and day 4–6 for 35 °C (a and b); day 10–15 (c and d).

decreasing light intensity from 500 to 50 $\mu\text{mol m}^{-2} \text{s}^{-1}$ (Table 2). High light intensity showed a clear negative effect on Fx accumulation. Several previous studies have reported higher Fx contents at lower light intensities (Gómez-Loredo et al., 2016; Li et al., 2019). However, the Fx productivity was the highest at 150 and 300 $\mu\text{mol m}^{-2} \text{s}^{-1}$ but lowest at 50 $\mu\text{mol m}^{-2} \text{s}^{-1}$. Different light intensities did not show clear effect on TFA and DHA content. However, the neutral lipids fraction of TFA increased from 3.45% to 52.32% with increasing light from 50 to 500 $\mu\text{mol m}^{-2} \text{s}^{-1}$ (Table 2). Neutral lipids are commonly accepted as energy storage compounds and can be induced by high light intensities (Solovchenko, 2012; Xiao et al., 2015).

Results from both temperature and light optimization experiments show that 30 °C and 300 $\mu\text{mol m}^{-2} \text{s}^{-1}$ are the optimal conditions to achieve the highest Fx productivity. These conditions are similar to the optimal growth conditions found for the original *T. lutea* by Gao et al. (2020a).

3.3. Comparing original and novel *Tisochrysis lutea* phenotypes

Scale and conditions (outdoor vs indoors) have a huge impact on growth and productivities (Benvenuti et al., 2016; De Vree et al., 2015). For this reason, and to be able to show the industrial potential of a novel phenotype, its performance needs to be evaluated under different scales as well as outdoors. In this section, both original and novel *T. lutea* were cultivated in parallel in Algaemists (0.4 L), indoor flat-panel PBRs (25 L) and outdoor tubular PBRs (190 L) to compare their performance at different scales, indoors and outdoors, under identical conditions

(Fig. 3). The Algaemist were operated under continuous chemostat mode with fixed dilution rate. The flat-panel PBRs were operated batch wise, and the tubular PBRs outdoors were operated under semi-continuous mode with a constant biomass concentration (1 g L⁻¹ AFDW).

3.3.1. Growth and biomass production

The biomass productivity of the novel *T. lutea* phenotype in the Algaemist continuous chemostat (0.4 L) was 1.9-fold higher than the original phenotype (Table 3). The biomass productivity of the novel phenotype was 4.1- and 4.5-fold higher than the original strain in flat-panel (25 L) and tubular (190 L) PBRs (Table 3). The improved biomass productivity can result from the lost flagella, since no energy is needed for swimming. These results show that the novel *T. lutea* is a robust strain with high biomass productivity. The biomass productivity (0.54 g L⁻¹ d⁻¹) obtained in tubular PBRs was the highest ever reported at outdoor conditions (Ippoliti et al., 2016b; Zhu et al., 2019).

The biomass productivity of the original strain decreased from 0.54 to 0.12 g L⁻¹ d⁻¹ AFDW during cultivation from 0.4 to 190 L (Table 3). One big challenge for microalgae outdoor production is contamination by grazers, which is an overlooked issue considering the high crash risk (Day, 2013; Huang et al., 2014). Due to nutritional value and digestibility, *T. lutea* has high contamination risk serving as feed for grazers (Gladue and Maxey, 1994; Jia-Yicao et al., 2019). In the present study, no grazers were found in Algaemist and flat-panel PBRs in the greenhouse but were found in outdoor tubular PBRs with the original *T. lutea* strain. During semi-continuous cultivation, no dilutions were

Table 1
Growth and biomass composition of the novel *Tisochrysis lutea* phenotype at different temperatures.

Temperature (°C)	15.8	20	25	30	35
μ (d ⁻¹)	0.05 ± 0.02 ^d	0.25 ± 0.02 ^b	0.29 ± 0.03 ^b	0.41 ± 0.08 ^a	0.11 ± 0.08 ^c
Biomass concentration (g L ⁻¹ AFDW)	3.04 ± 0.32 ^a	2.75 ± 0.18 ^{ab}	2.76 ± 0.02 ^{ab}	2.61 ± 0.15 ^{ab}	2.56 ± 0.03 ^b
Biomass productivity (g L ⁻¹ d ⁻¹ AFDW)	0.14 ± 0.05 ^d	0.72 ± 0.08 ^b	0.88 ± 0.05 ^{ab}	1.01 ± 0.14 ^a	0.38 ± 0.06 ^c
Fx content (mg g ⁻¹ AFDW)	4.06 ± 0.55 ^{ab}	3.69 ± 0.25 ^{bc}	4.68 ± 0.45 ^a	4.24 ± 0.41 ^{ab}	3.02 ± 0.39 ^c
Fx productivity (mg L ⁻¹ d ⁻¹)	0.55 ± 0.14 ^c	2.64 ± 0.26 ^b	4.24 ± 0.22 ^a	4.32 ± 1.02 ^a	1.21 ± 0.21 ^c
TFA content (mg g ⁻¹ AFDW)	107.07 ± 0.50 ^a	110.37 ± 0.99 ^a	108.61 ± 2.86 ^a	103.69 ± 3.42 ^a	73.92 ± 22.10 ^b
Polar lipids fraction (% TFA)	50.85 ± 10.35 ^b	54.42 ± 6.79 ^{ab}	58.77 ± 1.53 ^{ab}	68.46 ± 3.15 ^a	65.99 ± 0.20 ^{ab}
Neutral lipids fraction (% TFA)	49.15 ± 10.35 ^a	45.58 ± 6.79 ^{ab}	41.23 ± 1.53 ^{ab}	31.54 ± 3.15 ^b	34.01 ± 0.20 ^{ab}
TFA productivity (mg L ⁻¹ d ⁻¹)	11.73 ± 1.46 ^b	79.09 ± 9.21 ^a	95.17 ± 9.42 ^a	104.69 ± 13.60 ^a	28.97 ± 16.36 ^b
DHA content (mg g ⁻¹ AFDW)	13.06 ± 0.37 ^a	14.33 ± 0.36 ^a	12.71 ± 0.50 ^a	12.96 ± 0.07 ^a	8.67 ± 2.38 ^b
DHA productivity (mg L ⁻¹ d ⁻¹)	1.41 ± 0.12 ^b	10.24 ± 0.91 ^a	11.18 ± 1.41 ^a	13.10 ± 1.78 ^a	3.32 ± 1.20 ^b
QY (Fv/Fm)	0.61 ± 0.03 ^b	0.68 ± 0.01 ^a	0.71 ± 0.01 ^a	0.71 ± 0.01 ^a	0.53 ± 0.18 ^c

Values are shown as means ± SD. Means with different letters are significantly different ($p < 0.05$). Abbreviations: ash free dry weight (AFDW); fucoxanthin (Fx); total fatty acids (TFA); docosahexaenoic acid (DHA); quantum yield (QY).

Table 2
Growth and biomass composition of the selected novel *Tisochrysis lutea* phenotype at different light intensities.

Light intensity ($\mu\text{mol m}^{-2} \text{s}^{-1}$)	50	150	300	500
μ (d ⁻¹)	0.41 ± 0.02 ^{ab}	0.39 ± 0.01 ^b	0.40 ± 0.04 ^{ab}	0.42 ± 0.02 ^a
Biomass concentration (g L ⁻¹ AFDW)	0.67 ± 0.05 ^c	1.85 ± 0.06 ^b	1.96 ± 0.34 ^b	2.75 ± 0.21 ^a
Biomass productivity (g L ⁻¹ d ⁻¹ AFDW)	0.28 ± 0.02 ^c	0.71 ± 0.03 ^b	0.83 ± 0.09 ^b	1.12 ± 0.06 ^a
Fx content (mg g ⁻¹ AFDW)	6.66 ± 0.42 ^a	6.20 ± 0.25 ^a	4.65 ± 0.31 ^b	2.25 ± 0.17 ^c
Fx productivity (mg L ⁻¹ d ⁻¹)	1.82 ± 0.00 ^b	4.42 ± 0.41 ^a	3.84 ± 0.59 ^a	2.51 ± 0.32 ^b
TFA content (mg g ⁻¹ AFDW)	73.54 ± 4.35 ^c	88.01 ± 1.43 ^b	104.47 ± 7.54 ^a	98.43 ± 3.10 ^{ab}
Polar lipids fraction (% TFA)	96.55 ± 0.85 ^a	84.51 ± 2.74 ^b	58.11 ± 3.76 ^c	47.68 ± 0.91 ^d
Neutral lipids fraction (% TFA)	3.45 ± 0.85 ^d	15.49 ± 2.74 ^c	41.85 ± 3.76 ^b	52.32 ± 0.91 ^a
TFA productivity (mg L ⁻¹ d ⁻¹)	16.91 ± 6.43 ^c	62.61 ± 2.15 ^b	77.74 ± 11.09 ^b	109.99 ± 1.84 ^a
DHA content (mg g ⁻¹ AFDW)	8.95 ± 0.53 ^c	11.54 ± 0.25 ^b	13.20 ± 0.99 ^a	11.30 ± 0.48 ^b
DHA productivity (mg L ⁻¹ d ⁻¹)	2.06 ± 0.81 ^c	8.21 ± 0.29 ^b	9.82 ± 1.40 ^b	12.64 ± 1.49 ^a
QY (Fv/Fm)	0.73 ± 0.01 ^a	0.72 ± 0.01 ^a	0.73 ± 0.01 ^b	0.69 ± 0.02 ^c

Note: values are the means ± SD. Means with different letters are significantly different ($p < 0.05$). Abbreviations: ash free dry weight (AFDW); fucoxanthin (Fx); total fatty acids (TFA); docosahexaenoic acid (DHA); quantum yield (QY).

performed after two days due to decreased biomass concentration caused by grazers contamination/attack (ciliates). The original strain was cultivated at least 3 times during the last 2 years in tubular PBRs, and was always contaminated by ciliates, resulting in a low final biomass concentration (0.5–1 g L⁻¹). However, the outdoor biomass productivity of the novel *T. lutea* phenotype was stable and without grazers contamination. A longer cultivation (40 days) was performed with the novel *T. lutea* with different biomass concentrations (2 and 4 g L⁻¹; data not shown), also showing no grazer contaminations. It is reported that *Microcystis aeruginosa* and *Chlamydomonas reinhardtii* can aggregate, becoming larger, leading to consumption-resistance by grazers (Day, 2013). Therefore, the aggregated cells of the novel phenotype show an advantage in outdoor production. In addition, the fast growth rate helps developing a population advantage against the grazers, enhancing the contamination resistance.

3.3.2. Fucoxanthin and DHA production

The Fx content (5.51–10.73 mg g⁻¹) of the original *T. lutea* was higher than the novel phenotype (3.94–6.98 mg g⁻¹) cultivated in the different systems (Table 3; $p < 0.05$). However, the Fx productivity of the novel phenotype was 1.6-, 2.7-, and 3.1-fold higher than the original strain from 0.4 to 190 L. Fx productivity of both original and novel phenotypes showed a decrease from indoors to outdoors (76.6% and 54.8%, respectively). Compared to the original strain, the novel phenotype showed a lower decrease in Fx productivity. Fx productivity of the novel phenotype obtained at pilot scale outdoors (2.13 mg L⁻¹ d⁻¹; maximum light intensity 1500 $\mu\text{mol m}^{-2} \text{s}^{-1}$) was lower than some reported results (2.94–9.81 mg L⁻¹ d⁻¹) obtained indoors at laboratory scale and low light intensity (120 or 300 $\mu\text{mol m}^{-2} \text{s}^{-1}$) (Gao et al., 2020c; Li et al., 2019; Sun et al., 2019). However, it is the highest ever reported Fx productivity obtained at pilot scale outdoors. It is 8.8× higher than that obtained with *Navicula* sp. using an air-lift column photobioreactors outdoors (maximum light intensity 2700 $\mu\text{mol m}^{-2} \text{s}^{-1}$) (Telussa et al., 2019). The TFA and DHA content and productivity followed the same trends as Fx (Table 3). The outdoor DHA productivity at pilot scale (4.81 mg L⁻¹ d⁻¹) was higher than that obtained under indoor conditions with 2.5–6 L cultivation volume (1.1–4.3 mg L⁻¹ d⁻¹) (da Costa et al., 2017; Grant Burgess et al., 1993).

Besides pigments and lipids, other biochemical components, such as proteins and carbohydrates, could change in different phenotypes. To make a more complete characterization of the new phenotype, total proteins and carbohydrates were also analysed for both strains. Both original and novel phenotypes showed high protein content, reaching 523.07 and 399.83 mg g⁻¹ AFDW (Table 3). These were comparable with protein content (450 mg g⁻¹ DW) obtained at outdoor conditions using tubular PBRs (3.0 m³ capacity) (Ippoliti et al., 2016b). The total protein content of the novel phenotype was 52.25–84.64% of the original *T. lutea* content. The protein productivity followed the same trends as Fx, TFA and DHA productivities. The carbohydrates content of the novel phenotype (275.73–389.14 mg g⁻¹ AFDW) was significantly higher than the original phenotype (159.41–288.37 mg g⁻¹ AFDW) in all three cultivation conditions ($p < 0.05$). The carbohydrates productivity of the novel phenotype was 2.64-, 7.88-, and 9.12-fold higher than the original phenotype while increasing the cultivation volume from 0.4 to 190 L. The outdoor carbohydrates productivity (149.44 mg L⁻¹ d⁻¹) was 2.8–6.0 times as that obtained from two *T. lutea* strains cultivated indoors in flasks, and 1.1–2.2 folds as that with *Isochrysis zhangjiangensis* cultivated in a 600-mL glass air bubble column PBRs (da Costa et al., 2017; Wang et al., 2014). The novel *T. lutea* is an ideal carbohydrate-enriched bioresource (Wang et al., 2014). Overall, the selected novel *T. lutea* is a super strain with high biomass and valuable compounds productivities.

4. Conclusions

This work obtained a novel *T. lutea* by 2 rounds of continuous

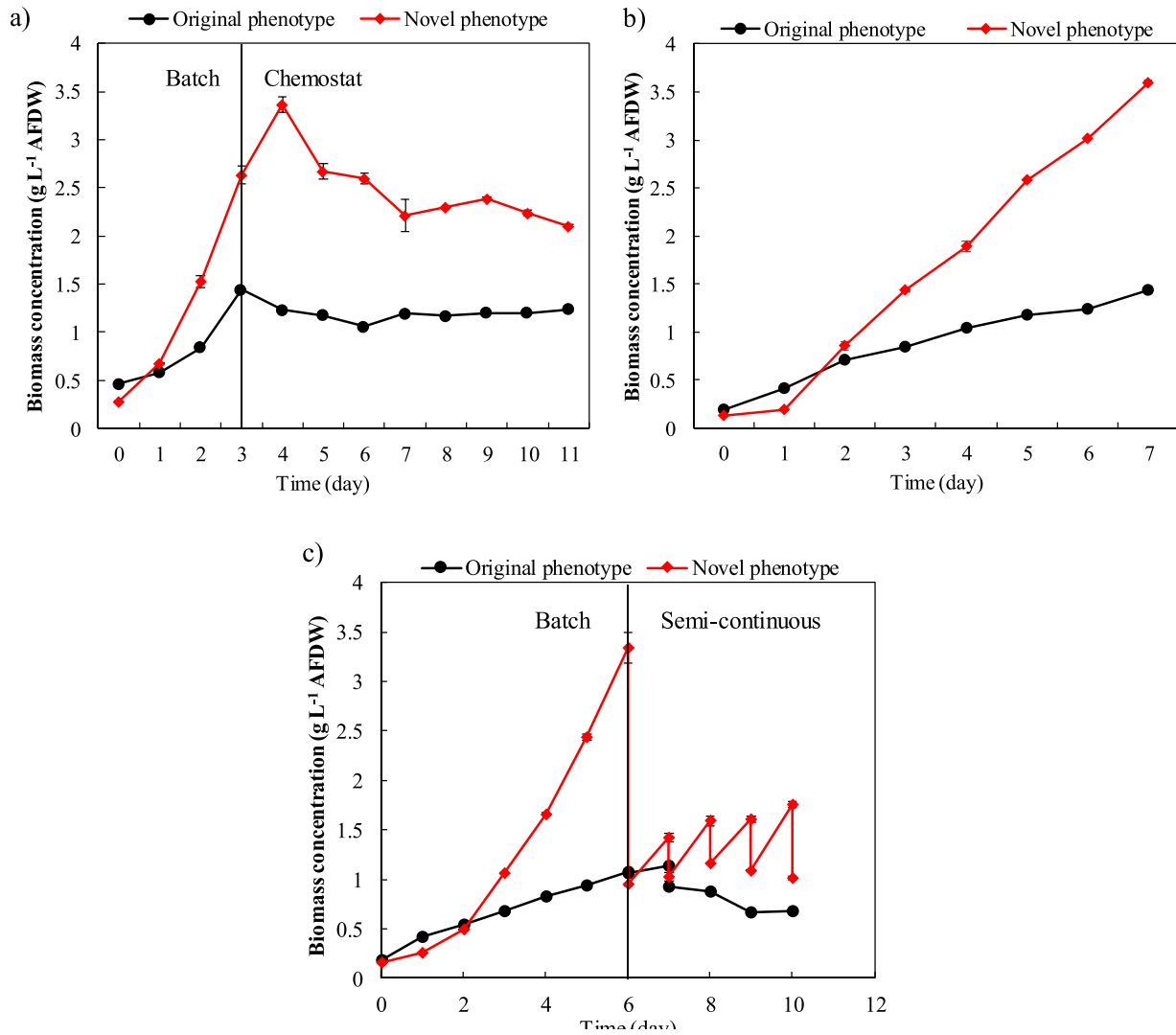


Fig. 3. Growth curves of original phenotype (●, black) and selected novel phenotype (◆, red) using different cultivation systems and modes. Note: a: Continuous chemostat cultivation using Algaemist (0.4 L); b: Batch cultivation using flat-panel photobioreactors (25 L); c: Semi-continuous cultivation using tubular photobioreactors (190 L). (For interpretation of the references to colour in this figure legend, the reader is referred to the web version of this article.)

Table 3
Comparison of original and selected phenotypes in growth and compounds details in different cultivation systems.

System	Algaemists		Flat-panel PBRs		Tubular PBRs	
Cultivation volume	0.4 L		25 L		190 L	
Cultivation mode	Continuous chemostat		Batch		Semi-continuous	
Strain	WT	NT	WT	NT	WT	NT
μ (d^{-1})	0.46 ± 0.03^a	0.48 ± 0.03^a	0.15 ± 0.00^b	0.49 ± 0.00^a	0.12 ± 0.04^b	0.51 ± 0.11^a
Biomass productivity ($g L^{-1} d^{-1}$ AFDW)	0.54 ± 0.03^b	1.05 ± 0.23^a	0.14 ± 0.00^b	0.57 ± 0.00^a	0.12 ± 0.04^b	0.54 ± 0.11^a
Fx content ($mg g^{-1}$ AFDW)	5.51 ± 0.35^a	4.51 ± 0.18^b	10.73 ± 0.12^a	6.98 ± 0.41^b	5.95 ± 1.13^a	3.94 ± 0.37^b
Fx productivity ($g L^{-1} d^{-1}$)	2.95 ± 0.19^b	4.71 ± 1.04^a	1.45 ± 0.05^b	3.97 ± 0.02^a	0.69 ± 0.24^b	2.13 ± 0.44^a
Lipid content ($mg g^{-1}$ AFDW)	123.64 ± 2.62^a	117.17 ± 9.66^b	156.32 ± 22.55^a	131.60 ± 26.80^a	157.39 ± 16.01^a	84.73 ± 12.30^b
Lipid productivity ($g L^{-1} d^{-1}$)	66.22 ± 4.31^b	122.61 ± 27.14^a	21.14 ± 0.66^a	74.83 ± 0.46^b	18.17 ± 6.39^a	45.92 ± 9.41^b
DHA content ($mg g^{-1}$ AFDW)	16.06 ± 0.28^a	12.02 ± 1.26^b	18.73 ± 5.31^a	8.58 ± 1.68^b	25.86 ± 3.97^a	8.87 ± 2.26^b
DHA productivity ($mg L^{-1} d^{-1}$)	8.60 ± 0.56^b	12.57 ± 2.78^a	2.53 ± 0.08^b	4.88 ± 0.03^a	2.98 ± 1.05^b	4.81 ± 0.98^a
Carbohydrates content ($mg g^{-1}$ AFDW)	288.37 ± 14.94^b	389.14 ± 46.70^a	159.41 ± 1.43^b	345.74 ± 14.11^a	163.94 ± 17.06^b	275.73 ± 45.36^a
Carbohydrates productivity ($mg L^{-1} d^{-1}$)	154.44 ± 10.05^b	407.24 ± 90.13^a	21.56 ± 0.67^b	196.62 ± 1.2^a	18.92 ± 6.65^b	149.44 ± 30.61^a
Protein content ($mg g^{-1}$ AFDW)	339.98 ± 61.58^a	196.38 ± 33.53^b	472.42 ± 1.58^a	399.83 ± 42.53^b	523.07 ± 4.88^a	273.31 ± 6.50^b
Protein productivity ($g L^{-1} d^{-1}$)	182.08 ± 11.85	205.51 ± 45.48	63.89 ± 1.99^b	227.37 ± 1.39^a	60.37 ± 21.23^b	148.13 ± 30.34^a

Note: values are the means \pm SD. Means with different letters are significantly different ($p < 0.05$). Abbreviations: ash free dry weight (AFDW); fucoxanthin (Fx); total fatty acids (TFA); docosahexaenoic acid (DHA); quantum yield (QY).

growing at low light combined with FACS selection. The strain formed cell aggregates, lost flagella and showed a stable phenotype after 15 months. Continuous experiments were conducted to obtain the optimal growth temperature (30 °C) and light intensity (300 $\mu\text{mol m}^{-2} \text{s}^{-1}$). Compared with the original phenotype, this new phenotype showed higher biomass, fucoxanthin and DHA productivities indoors and outdoors (0.4–190 L). The novel phenotype had the highest ever reported outdoor biomass and Fx productivities, which can be applied in industry to lower fucoxanthin and DHA production costs.

CRedit authorship contribution statement

Fengzheng Gao: Investigation, Methodology, Formal analysis, Data curation, Software, Visualization, Writing - original draft, Writing - review & editing. **Marta Sá:** Investigation, Methodology, Data curation, Writing - review & editing. **Iago Teles Dominguez Cabanelas:** Project administration, Formal analysis, Methodology, Supervision, Writing - review & editing. **René H. Wijffels:** Project administration, Supervision, Writing - review & editing. **Maria J. Barbosa:** Project administration, Formal analysis, Funding acquisition, Methodology, Supervision, Writing - review & editing.

Declaration of Competing Interest

The authors declare that they have no known competing financial interests or personal relationships that could have appeared to influence the work reported in this paper.

Acknowledgements

This research is part of the MAGNIFICENT project, funded by the Bio Based Industries Joint Undertaking under the European Union's Horizon 2020 research and innovation program (grant agreement No. 745754).

Appendix A. Supplementary data

Supplementary data to this article can be found online at <https://doi.org/10.1016/j.biortech.2021.124725>.

References

- Bendif, E.M., Probert, I., Schroeder, D.C., de Vargas, C., 2013. On the description of *Tisochrysis lutea* gen. nov. sp. nov. and *Isochrysis nuda* sp. nov. in the Isochrysidales, and the transfer of Dicrateria to the Prymnesiales (Haptophyta). *J. Appl. Phycol.* <https://doi.org/10.1007/s10811-013-0037-0>.
- Benvenuti, G., Bosma, R., Ji, F., Lamers, P., Barbosa, M.J., Wijffels, R.H., 2016. Batch and semi-continuous microalgal TAG production in lab-scale and outdoor photobioreactors. *J. Appl. Phycol.* <https://doi.org/10.1007/s10811-016-0897-1>.
- Cabanelas, I.T.D., Zwart, M.V.D., Kleinegris, D.M.M., Barbosa, M.J., Wijffels, R.H., 2015. Rapid method to screen and sort lipid accumulating microalgae. *Bioresour. Technol.* 184, 47–52. <https://doi.org/10.1016/j.biortech.2014.10.057>.
- Cabanelas, I.T.D., Van Der Zwart, M., Kleinegris, D.M.M., Wijffels, R.H., Barbosa, M.J., 2016. Sorting cells of the microalga *Chlorococcum littorale* with increased triacylglycerol productivity. *Biotechnol. Biofuels* 9, 1–12. <https://doi.org/10.1186/s13068-016-0595-x>.
- Colombo, S.M., Rodgers, T.F.M., Diamond, M.L., Bazinet, R.P., Arts, M.T., 2020. Projected declines in global DHA availability for human consumption as a result of global warming. *Ambio* 49, 865–880. <https://doi.org/10.1007/s13280-019-01234-6>.
- da Costa, F., Le Grand, F., Quéré, C., Bougaran, G., Cadoret, J.P., Robert, R., Soudant, P., 2017. Effects of growth phase and nitrogen limitation on biochemical composition of two strains of *Tisochrysis lutea*. *Algal Research* 27, 177–189. <https://doi.org/10.1016/j.algal.2017.09.003>.
- Day, J.G., 2013. Grazers: the overlooked threat to the sustained production of future algal biofuels. *Biofuels*. <https://doi.org/10.4155/bfs.13.29>.
- de Vree, J.H., Bosma, R., Janssen, M., Barbosa, M.J., Wijffels, R.H., 2015. Comparison of four outdoor pilot-scale photobioreactors. *Biotechnol. Biofuels*. <https://doi.org/10.1186/s13068-015-0400-2>.
- Dubois, M., Gilles, K.A., Hamilton, J.K., Rebers, P.A., Smith, F., 1956. Colourimetric Method for Determination of Sugars and Related Substances. *Chem. Anal.* <https://doi.org/10.1021/ac60111a017>.
- Fung, A., Hamid, N., Lu, J., 2013. Fucoxanthin content and antioxidant properties of *Undaria pinnatifida*. *Food Chem.* <https://doi.org/10.1016/j.foodchem.2012.09.024>.
- Gao, F., Sá, M., Cabanelas, I.T., Wijffels, R.H., Barbosa, M.J., 2020a. Production and monitoring of biomass and fucoxanthin with brown microalgae under outdoor conditions. *Biotechnol. Bioeng.* <https://doi.org/10.1002/bit.27657>.
- Gao, F., Teles (Cabanelas, ITD), I., Ferrer-Ledo, N., Wijffels, R.H., Barbosa, M.J., 2020b. Production and high throughput quantification of fucoxanthin and lipids in *Tisochrysis lutea* using single-cell fluorescence. *Bioresour. Technol.* <https://doi.org/10.1016/j.biortech.2020.124104>.
- Gao, F., Teles (Cabanelas, ITD), I., Wijffels, R.H., Barbosa, M.J., 2020c. Process optimization of fucoxanthin production with *Tisochrysis lutea*. *Bioresour. Technol.* <https://doi.org/10.1016/j.biortech.2020.123894>.
- Gao, F., Wooldschot, S., Cabanelas, I.T.D., Wijffels, R.H., Barbosa, M.J., 2021. Light spectra as triggers for sorting improved strains of *Tisochrysis lutea*. *Bioresour. Technol.* <https://doi.org/10.1016/j.biortech.2020.124434>.
- Gladue, R.M., Maxey, J.E., 1994. Microalgal feeds for aquaculture. *J. Appl. Phycol.* <https://doi.org/10.1007/BF02186067>.
- Gómez-Loredo, A., Benavides, J., Rito-Palomares, M., 2016. Growth kinetics and fucoxanthin production of *Phaeodactylum tricornutum* and *Isochrysis galbana* cultures at different light and agitation conditions. *J. Appl. Phycol.* 28, 849–860. <https://doi.org/10.1007/s10811-015-0635-0>.
- Grant Burgess, J., Iwamoto, K., Miura, Y., Takano, H., Matsunaga, T., 1993. An optical fibre photobioreactor for enhanced production of the marine unicellular alga *Isochrysis* aff. *galbana* T-Iso (UTEX LB 2307) rich in docosahexaenoic acid. *Appl. Microbiol. Biotechnol.* 39, 456–459. <https://doi.org/10.1007/BF00205032>.
- Guedes, A.C., Amaro, H.M., Malcata, F.X., 2011. Microalgae as sources of carotenoids. *Mar. Drugs* 9, 625–644. <https://doi.org/10.3390/md9040625>.
- Huang, Y., Liu, J., Li, L., Pang, T., Zhang, L., 2014. Efficacy of binary combinations of botanical pesticides for rotifer elimination in microalgal cultivation. *Bioresour. Technol.* <https://doi.org/10.1016/j.biortech.2013.11.098>.
- Hulatt, C.J., Wijffels, R.H., Bolla, S., Kiron, V., 2017. Production of fatty acids and protein by nanochloropsis in flat-plate photobioreactors. *PLoS One* 12, 1–17. <https://doi.org/10.1371/journal.pone.0170440>.
- Ippoliti, D., Gómez, C., del Mar Morales-Amaral, M., Pistocchi, R., Fernández-Sevilla, J. M., Acien, F.G., 2016a. Modeling of photosynthesis and respiration rate for *Isochrysis galbana* (T-Iso) and its influence on the production of this strain. *Bioresour. Technol.* 203, 71–79. <https://doi.org/10.1016/j.biortech.2015.12.050>.
- Ippoliti, D., González, A., Martín, I., Sevilla, J.M.F., Pistocchi, R., Acien, F.G., 2016b. Outdoor production of *Tisochrysis lutea* in pilot-scale tubular photobioreactors. *J. Appl. Phycol.* 28, 3159–3166. <https://doi.org/10.1007/s10811-016-0856-x>.
- Ishika, T., Moheimani, N.R., Bahri, P.A., Laird, D.W., Blair, S., Parlevliet, D., 2017. Halo-adapted microalgae for fucoxanthin production: Effect of incremental increase in salinity. *Algal Research* 28, 66–73. <https://doi.org/10.1016/j.algal.2017.10.002>.
- Jia-Yicao, J.Y., Kong, Z.Y., Zhang, Y.F., Ling, T., Xu, J.L., Liao, K., Zhou, C.X., Yan, X.J., 2019. Bacterial community diversity and screening of growth-affecting bacteria from *Isochrysis galbana* following antibiotic treatment. *Front. Microbiol.* 10, 1–11. <https://doi.org/10.3389/fmicb.2019.00994>.
- Joel, J., 2016. Global fucoxanthin market 2016 industry trends, sales, supply, demand, analysis and forecast to 2021. *Anal. Forecast.*
- Li, Y., Sun, H., Wu, T., Fu, Y., He, Y., Mao, X., Chen, F., 2019. Storage carbon metabolism of *Isochrysis zhangjiangensis* under different light intensities and its application for co-production of fucoxanthin and stearidonic acid. *Bioresour. Technol.* 282, 94–102. <https://doi.org/10.1016/j.biortech.2019.02.127>.
- Lim, D.K.Y., Schuhmann, H., Sharma, K., Schenk, P.M., 2015. Isolation of High-Lipid *Tetraselmis suecica* Strains Following Repeated UV-C Mutagenesis, FACS, and High-Throughput Growth Selection. *Bioenerg. Res.* 8, 750–759. <https://doi.org/10.1007/s12155-014-9553-2>.
- Liu, J., Sommerfeld, M., Hu, Q., 2013. Screening and characterization of *Isochrysis* strains and optimization of culture conditions for docosahexaenoic acid production. *Appl. Microbiol. Biotechnol.* 97, 4785–4798. <https://doi.org/10.1007/s00253-013-4749-5>.
- Lowry, O.H., Rosebrough, N.J., Farr, A.L., Randall, R.J., 1951. Protein measurement with the Folin phenol reagent. *J. Biol. Chem.* [https://doi.org/10.1016/0922-338X\(96\)89160-4](https://doi.org/10.1016/0922-338X(96)89160-4).
- Lu, X., Sun, H., Zhao, W., Cheng, K.W., Chen, F., Liu, B., 2018. A hetero-photoautotrophic two-stage cultivation process for production of fucoxanthin by the marine diatom *Nitzschia laevis*. *Mar. Drugs* 16. <https://doi.org/10.3390/md16070219>.
- Maeda, H., Fukuda, S., Izumi, H., Saga, N., 2018. Anti-oxidant and fucoxanthin contents of brown alga *Ishimozuku (Sphaerotrichia divaricata)* from the west coast of aomori, Japan. *Mar. Drugs* 16, 1–10. <https://doi.org/10.3390/md16080255>.
- Mendoza, H., de la Jara, A., Freijanes, K., Carmona, L., Ramos, A.A., de Sousa Duarte, V., Serafim Varela, J.C., 2008. Characterization of Dunaliella salina strains by flow cytometry: a new approach to select carotenoid hyperproducing strains. *Electron. J. Biotechnol.* 11. <https://doi.org/10.2225/vol11-issue4-fulltext-2>.
- Mishra, N.N., Rubio, A., Nast, C.C., Bayer, A.S., 2012. Differential Adaptations of Methicillin-Resistant Staphylococcus aureus to Serial in Vitro Passage in Daptomycin: Evolution of Daptomycin Resistance and Role of Membrane Carotenoid Content and Fluidity. *J. Microbiol. Int.* <https://doi.org/10.1155/2012/683450>.
- Pereira, H., Barreira, L., Mozes, A., Florindo, C., Polo, C., Duarte, C.V., Custódio, L., Varela, J., 2011. Microplate-based high throughput screening procedure for the isolation of lipid-rich marine microalgae. *Biotechnol. Biofuels* 4, 61. <https://doi.org/10.1186/1754-6834-4-61>.
- Pereira, H., Schulze, P.S.C., Schüler, L.M., Santos, T., Barreira, L., Varela, J., 2018. Fluorescence activated cell-sorting principles and applications in microalgal biotechnology. *Algal Research* 30, 113–120. <https://doi.org/10.1016/j.algal.2017.12.013>.
- Picardo, M.C., De Medeiros, J.L., Monteiro, J.G.M., Chaloub, R.M., Giordano, M., De Queiroz Fernandes Araújo, O., 2013. A methodology for screening of microalgae as a

- decision making tool for energy and green chemical process applications. *Clean Technol. Environ. Policy* 15, 275–291. <https://doi.org/10.1007/s10098-012-0508-z>.
- Solovchenko, A.E., 2012. Physiological role of neutral lipid accumulation in eukaryotic microalgae under stresses. *Russ. J. Plant Physiol.* 59, 167–176. <https://doi.org/10.1134/S1021443712020161>.
- Sukenik, A., Zmora, O., Carmeli, Y., 1993. Biochemical quality of marine unicellular algae with special emphasis on lipid composition. II. *Nannochloropsis* sp. *Aquaculture* 117, 313–326. [https://doi.org/10.1016/0044-8486\(93\)90328-V](https://doi.org/10.1016/0044-8486(93)90328-V).
- Sun, Z., Wang, X., Liu, J., 2019. Screening of *Isochrysis* strains for simultaneous production of docosahexaenoic acid and fucoxanthin. *Algal Research* 41, 101545. <https://doi.org/10.1016/j.algal.2019.101545>.
- Swanson, D., Block, R., Mousa, S.A., 2012. Omega-3 Fatty Acids EPA and DHA : Health. *J. Adv. Nutr.* 3, 1–7. <https://doi.org/10.3945/an.111.000893.Omega-3>.
- Telussa, I., Rusnadi, Zeily Nurachman, 2019. Dynamics of β -carotene and fucoxanthin of tropical marine *Navicula* sp. as a response to light stress conditions. *Algal Research* 41, 101530. <https://doi.org/10.1016/j.algal.2019.101530>.
- Terasaki, M., Narayan, B., Kamogawa, H., Nomura, M., Stephen, N.M., Kawagoe, C., Hosokawa, M., Miyashita, K., 2012. Carotenoid Profile of Edible Japanese Seaweeds: An Improved HPLC Method for Separation of Major Carotenoids. *J. Aquat. Food Prod. Technol.* 21, 468–479. <https://doi.org/10.1080/10498850.2011.610025>.
- Verma, P., Kumar, M., Mishra, G., Sahoo, D., 2017. Multivariate analysis of fatty acid and biochemical constituents of seaweeds to characterize their potential as bioresource for biofuel and fine chemicals. *Bioresour. Technol.* 226, 132–144. <https://doi.org/10.1016/j.biortech.2016.11.044>.
- Wang, H.T., Yao, C.H., Ai, J.N., Cao, X.P., Xue, S., Wang, W., Liang, 2014. Identification of carbohydrates as the major carbon sink of the marine microalga *Isochrysis zhangjiangensis* (Haptophyta) and optimization of its productivity by nitrogen manipulation. *Bioresour. Technol.* 171, 298–304. <https://doi.org/10.1016/j.biortech.2014.08.090>.
- Xiao, Y., Zhang, J., Cui, J., Yao, X., Sun, Z., Feng, Y., Cui, Q., 2015. Simultaneous accumulation of neutral lipids and biomass in *Nannochloropsis oceanica* IMET1 under high light intensity and nitrogen replete conditions. *Algal Research* 11, 55–62. <https://doi.org/10.1016/j.algal.2015.05.019>.
- Yamada, K., Suzuki, H., Takeuchi, T., Kazama, Y., Mitra, S., Abe, T., Goda, K., Suzuki, K., Iwata, O., 2016. Efficient selective breeding of live oil-rich *Euglena gracilis* with fluorescence-activated cell sorting. *Sci. Rep.* 6, 2–9. <https://doi.org/10.1038/srep26327>.
- Yen Doan, T.T., Obbard, J.P., 2011. Enhanced lipid production in *Nannochloropsis* sp. using fluorescence-activated cell sorting. *GCB Bioenergy* 3, 264–270. <https://doi.org/10.1111/j.1757-1707.2010.01076.x>.
- Zailanie, K., Sukoso, 2014. Study on of Fucoxanthin Content and its Identification in Brown Algae from Padike Vilage Talango District, Madura Islands. *J. Life Sci. Biomed.*
- Zhu, C., Han, D., Li, Y., Zhai, X., Chi, Z., Zhao, Y., Cai, H., 2019. Cultivation of aquaculture feed *Isochrysis zhangjiangensis* in low-cost wave driven floating photobioreactor without aeration device. *Bioresour. Technol.* 293, 122018. <https://doi.org/10.1016/j.biortech.2019.122018>.